Supplementary Material

The influence of the matrix on the apatite forming ability of calcium containing polydimethylsiloxane-based cements for endodontics

Paola Taddei, Michele Di Foggia, Fausto, Zamparini, Carlo Prati, Maria Giovanna Gandolfi

Table S1. Wavenumbers and assignments [20-25] of the main IR bands detected in the spectra of the commercial cements (orange and white pastes, just mixed sealers).

Wavenumbers / cm^{-1}	Assignments
3055	=CH stretching
2963	CH_3 antisymmetric stretching
2905	CH_3 symmetric stretching
2160	Si-H stretching
1600	C=C stretching
1450	CH_3 antisymmetric bending
1411	CH_3 symmetric bending
1258	CH_3 symmetric deformation
1078	antisymmetric Si-O-Si stretching
1010	symmetric Si-O-Si stretching
930	non-bridging oxygen, $Si–O_{NBO}$ stretching mode
910	Si-H bending
866	CH_3 symmetric rocking
790	CH_3 antisymmetric rocking, Si-C antisymmetric stretching
740	Si-C symmetric stretching, Si-C antisymmetric bending, Si-O bending, monoclinic ZrO_2
572	monoclinic ZrO_2
490	monoclinic ZrO_2
450	monoclinic ZrO_2

Table S2. Wavenumbers and assignments [21,24,27-29] of the main Raman bands detected in the FT-Raman spectra of the commercial cements (orange and white pastes, just mixed sealers).

Wavenumbers / cm^{-1}	Assignments
3055	=CH stretching
2967	CH_3 antisymmetric stretching
2908	CH_3 symmetric stretching
2870	CH_3 symmetric stretching
1670	C=C stretching guttapercha
1600	C=C stretching
1411	CH_3 symmetric bending
1265	CH_3 symmetric deformation
1080	Si-O-Si stretching of SiO_4 tetrahedra
960-940	PO_4 stretching
861	CH_3 symmetric rocking
790	CH_3 antisymmetric rocking, Si-C antisymmetric stretching
755	Si-C symmetric stretching, Si-C antisymmetric bending, Si-O bending, monoclinic ZrO_2
710	Si-C symmetric stretching
690	Si-CH_3 symmetric rocking
638	monoclinic ZrO_2
616	monoclinic ZrO_2
559	monoclinic ZrO_2
537	monoclinic ZrO_2
500	monoclinic ZrO_2
476	monoclinic ZrO_2
435	ZnO
382	monoclinic ZrO_2
347	monoclinic ZrO_2
334	monoclinic ZrO_2
306	monoclinic ZrO_2
221	monoclinic ZrO_2
191	monoclinic ZrO_2
179	monoclinic ZrO_2

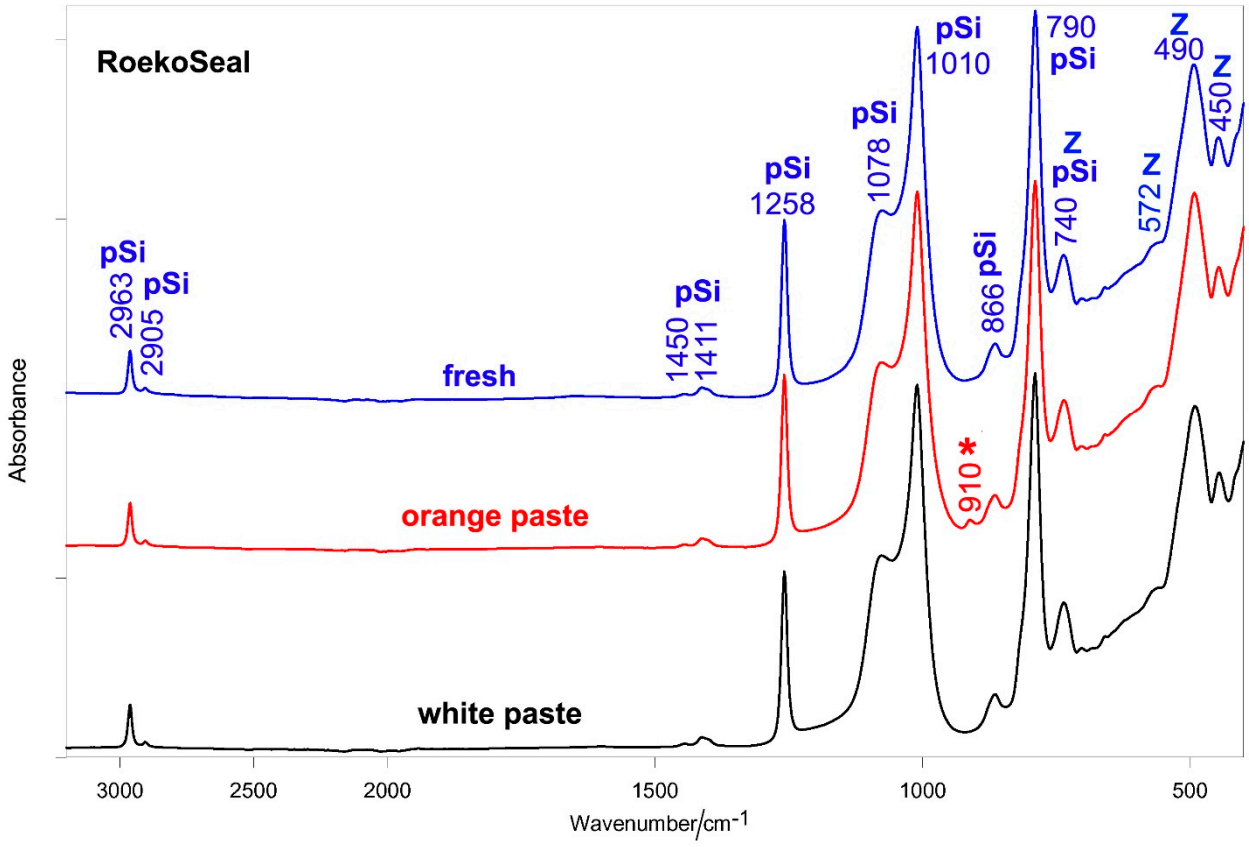

Figure S1. Average IR spectrum of fresh (i.e. just mixed) RoekoSeal; the spectra of its white and orange components are reported for comparison. The spectra are normalized to the absorbance of the 2963 cm^{-1} band. The bands assignable to polydimethylsiloxane (pSi) and monoclinic zirconia (Z) are indicated together with those specifically assigned to Si-H bonds (*).

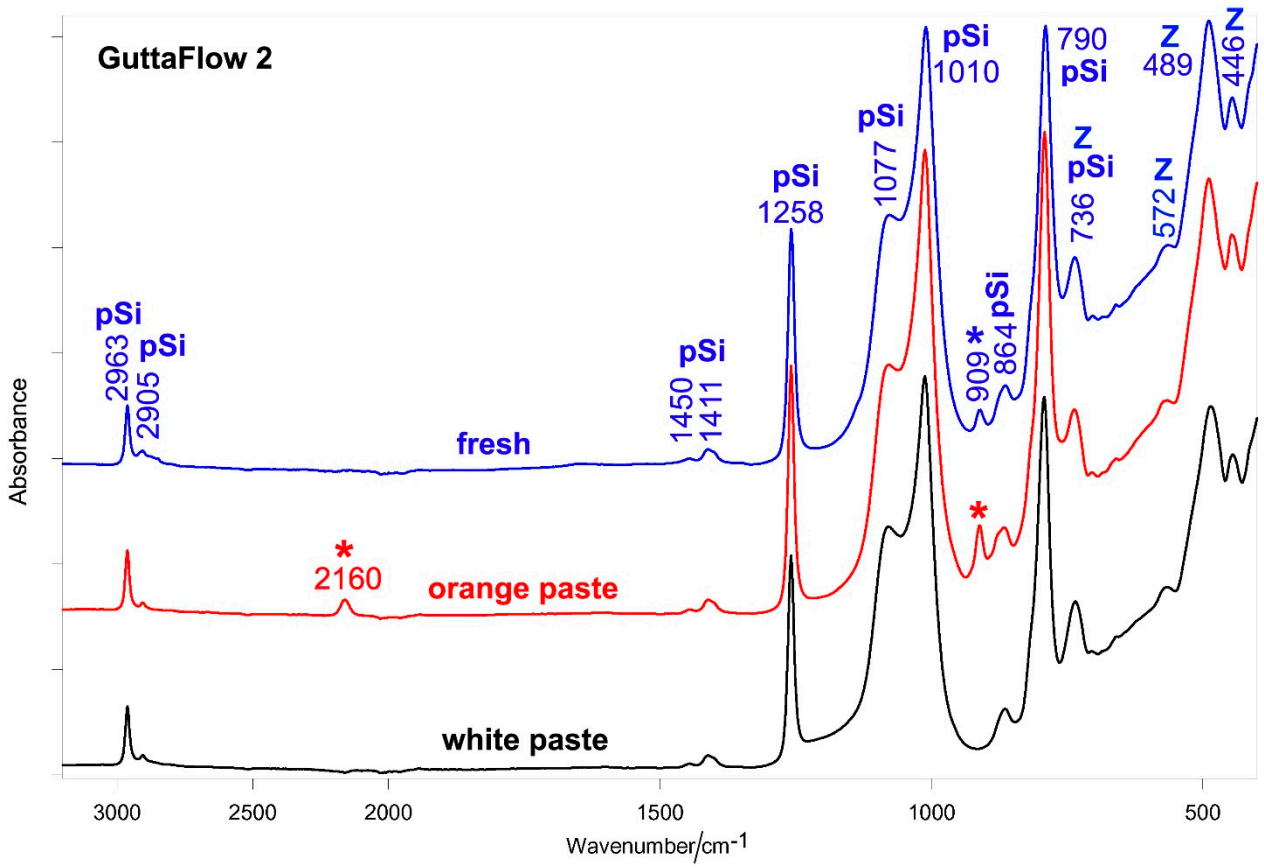

Figure S2. Average IR spectrum of fresh (i.e. just mixed) GuttaFlow 2; the spectra of its white and orange components are reported for comparison. The spectra are normalized to the absorbance of the 2963 cm^{-1} band. The bands assignable to polydimethylsiloxane (pSi) and monoclinic zirconia (Z) are indicated together with those specifically assigned to Si-H bonds (*).

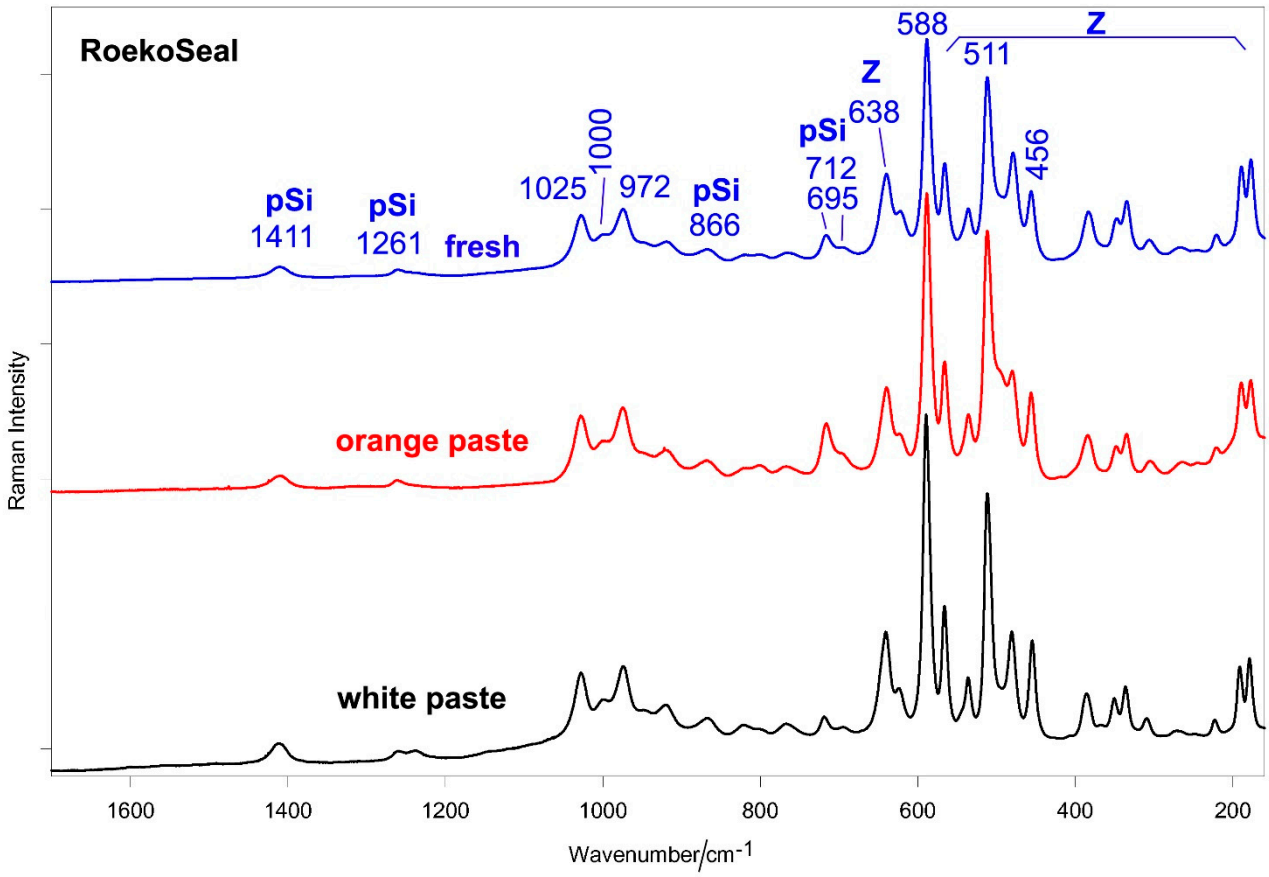

Figure S3. Average micro-Raman spectra of fresh (i.e. just mixed) RoekoSeal, its white and orange pastes. The spectra are normalized to the intensity of the 638 cm^{-1} band. The bands assignable to monoclinic zirconia (Z) and polydimethylsiloxane (pSi) are indicated.

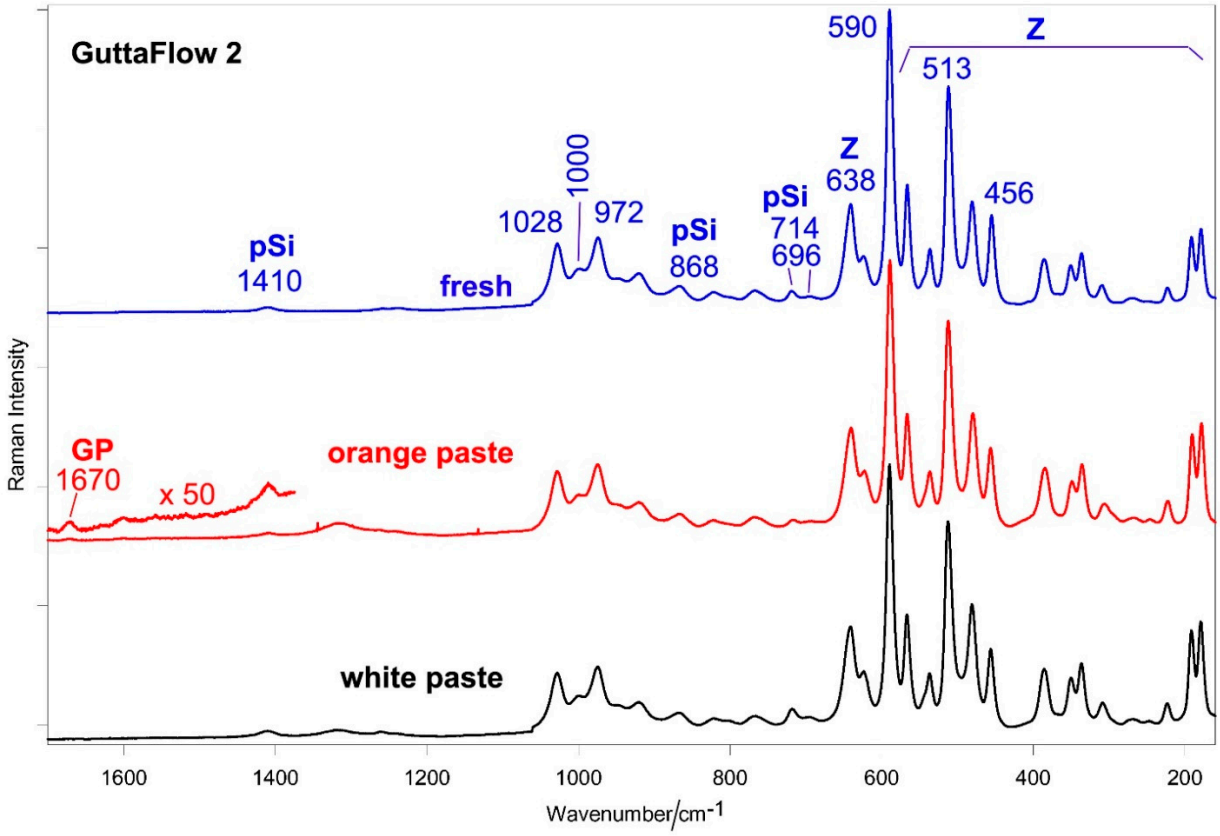

Figure S4. Average micro-Raman spectra of fresh (i.e. just mixed) GuttaFlow 2, its white and orange pastes. The spectra are normalized to the intensity of the 638 cm^{-1} band. The bands assignable to monoclinic zirconia (Z), polydimethylsiloxane (pSi) and guttapercha (GP) are indicated.

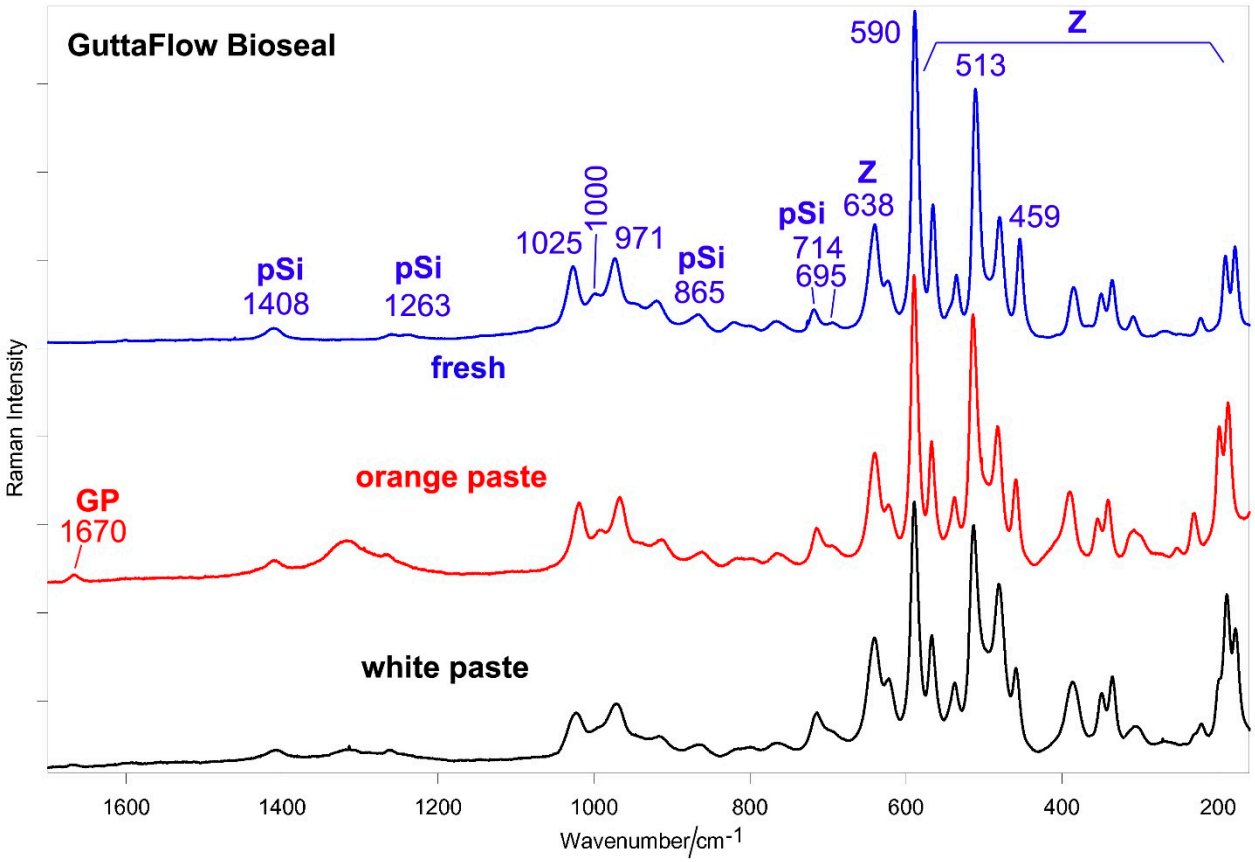

Figure S5. Average micro-Raman spectra of fresh (i.e. just mixed) GuttaFlow Bioseal, its white and orange pastes. The spectra are normalized to the intensity of the 638 cm^{-1} band. The bands assignable to monoclinic zirconia (Z), polydimethylsiloxane (pSi) and guttapercha (GP) are indicated.

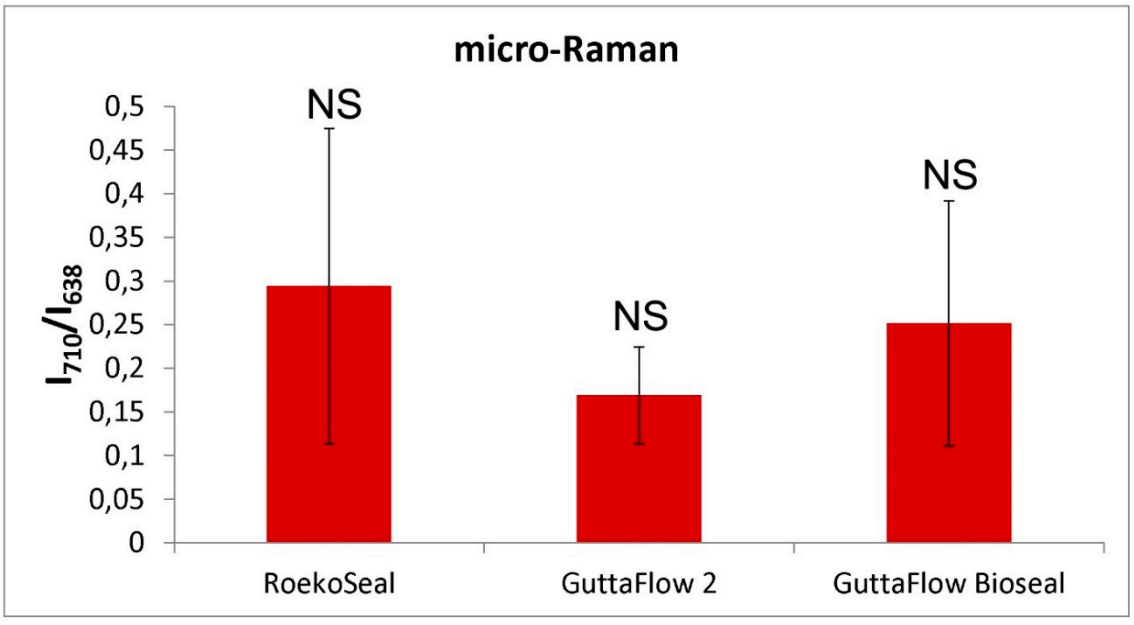

Figure S6. I_{710}/I_{638} intensity ratio (average ± standard deviation) as calculated from the micro-Raman spectra of fresh commercial sealers under study. No statistically significant differences were observed between the values (NS, $P > 0.05$).

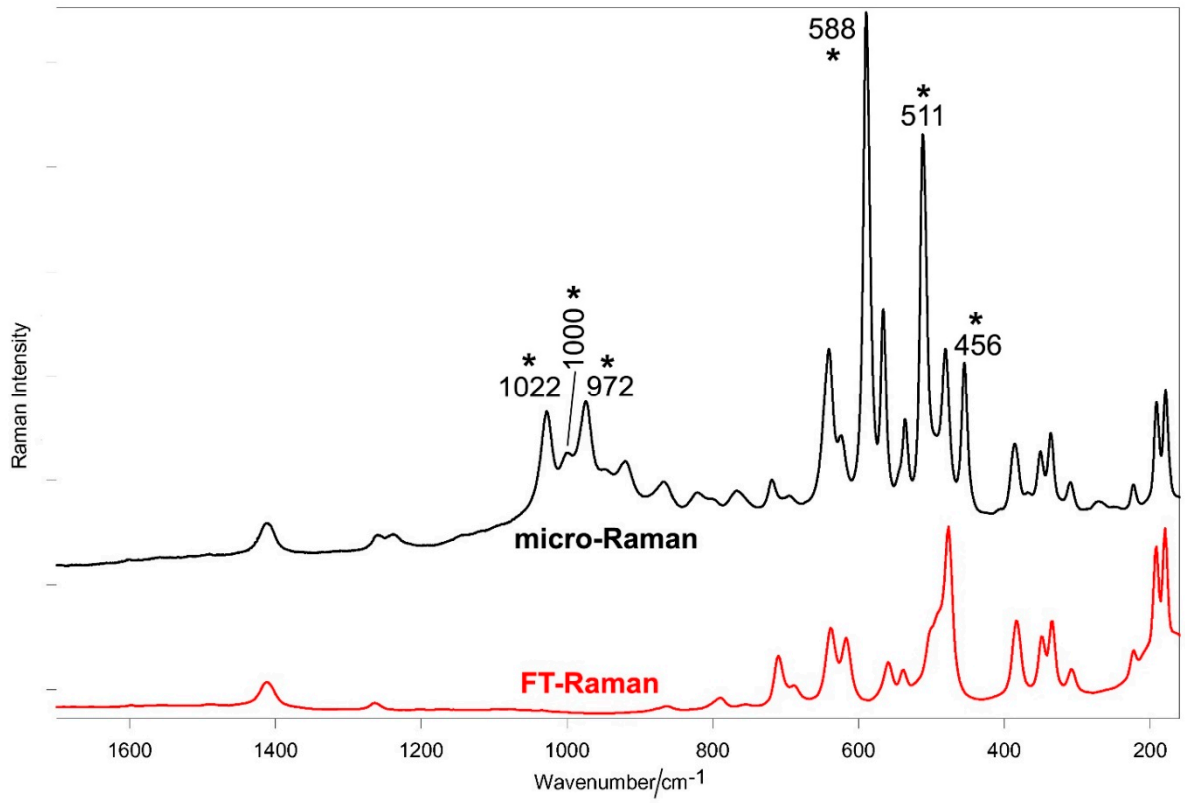

Figure S7. Average FT-Raman and micro-Raman spectra of white paste of RoekoSeal. The bands observed only in the micro-Raman spectrum are indicated with an asterisk.

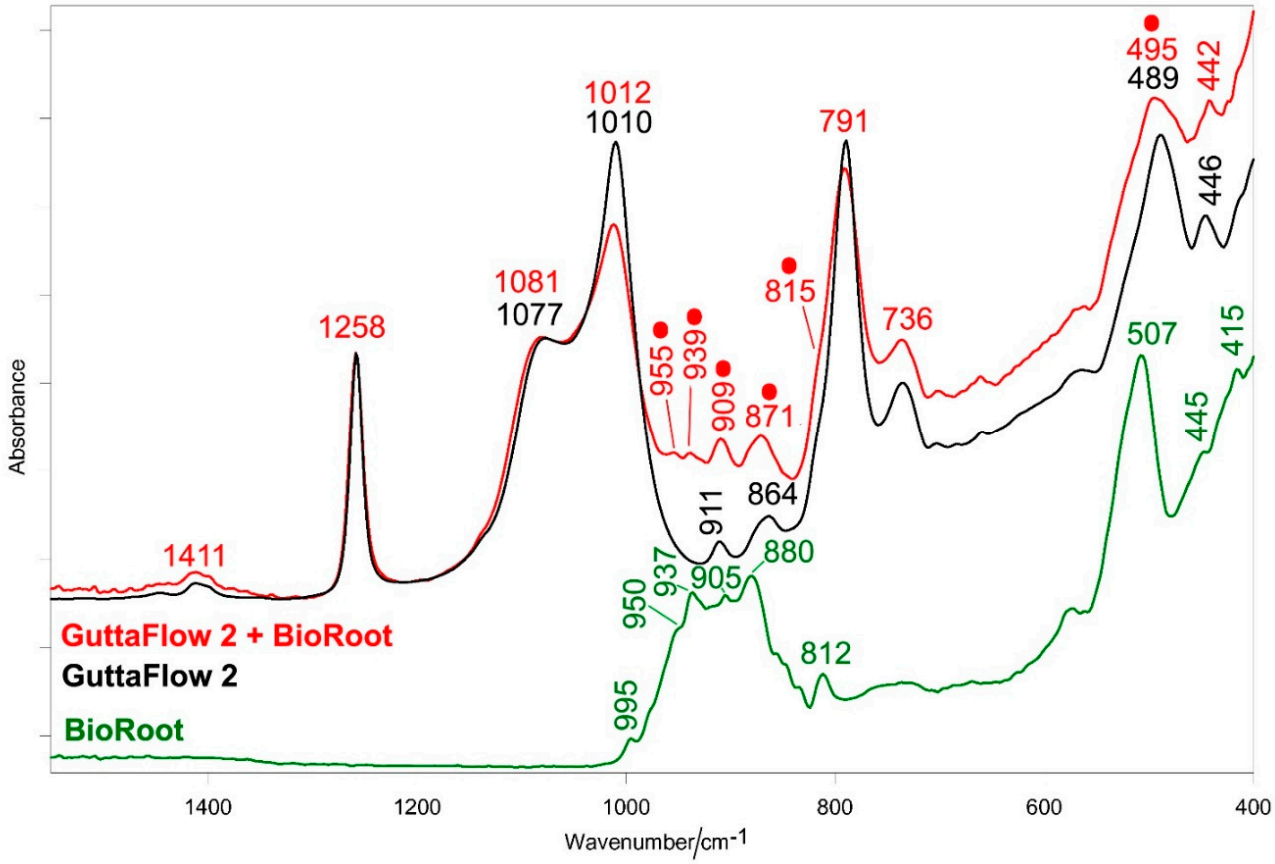

Figure S8. Average IR spectra of fresh GuttaFlow 2 + 20% BioRoot RCS and Guttaflow 2, normalized to the absorbance of the 1258 cm^{-1} band. The spectrum of BioRoot RCS is reported for comparison; spectral features assignable to it are indicated with a circle.

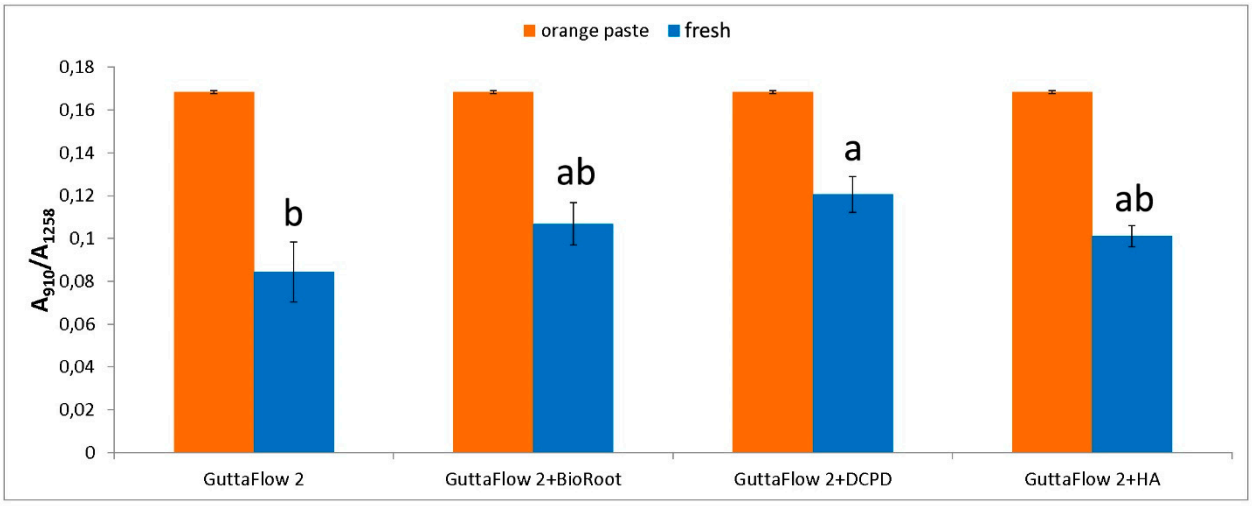

Figure S9. A_{910}/A_{1258} absorbance ratio (average ± standard deviation) as calculated from the IR spectra of the orange paste and fresh samples of the doped sealers under study (GuttaFlow 2 is reported for comparison). Different letters represent statistically significant differences ($P < 0.05$) between the fresh samples.

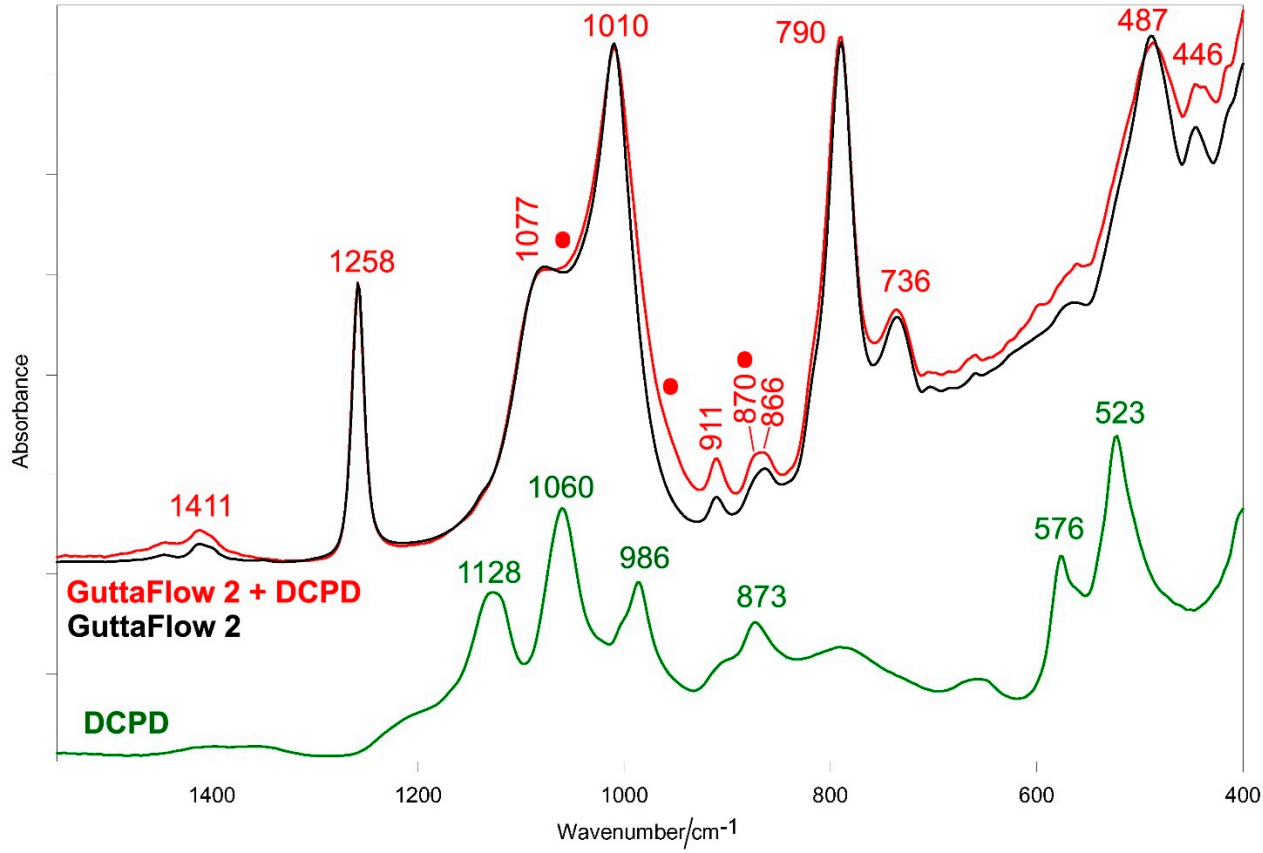

Figure S10. Average IR spectra of fresh GuttaFlow 2 + 20% DCPD and Guttaflow 2, normalized to the absorbance of the 1258 cm^{-1} band. The spectrum of DCPD is reported for comparison; spectral features assignable to it are indicated with a circle.

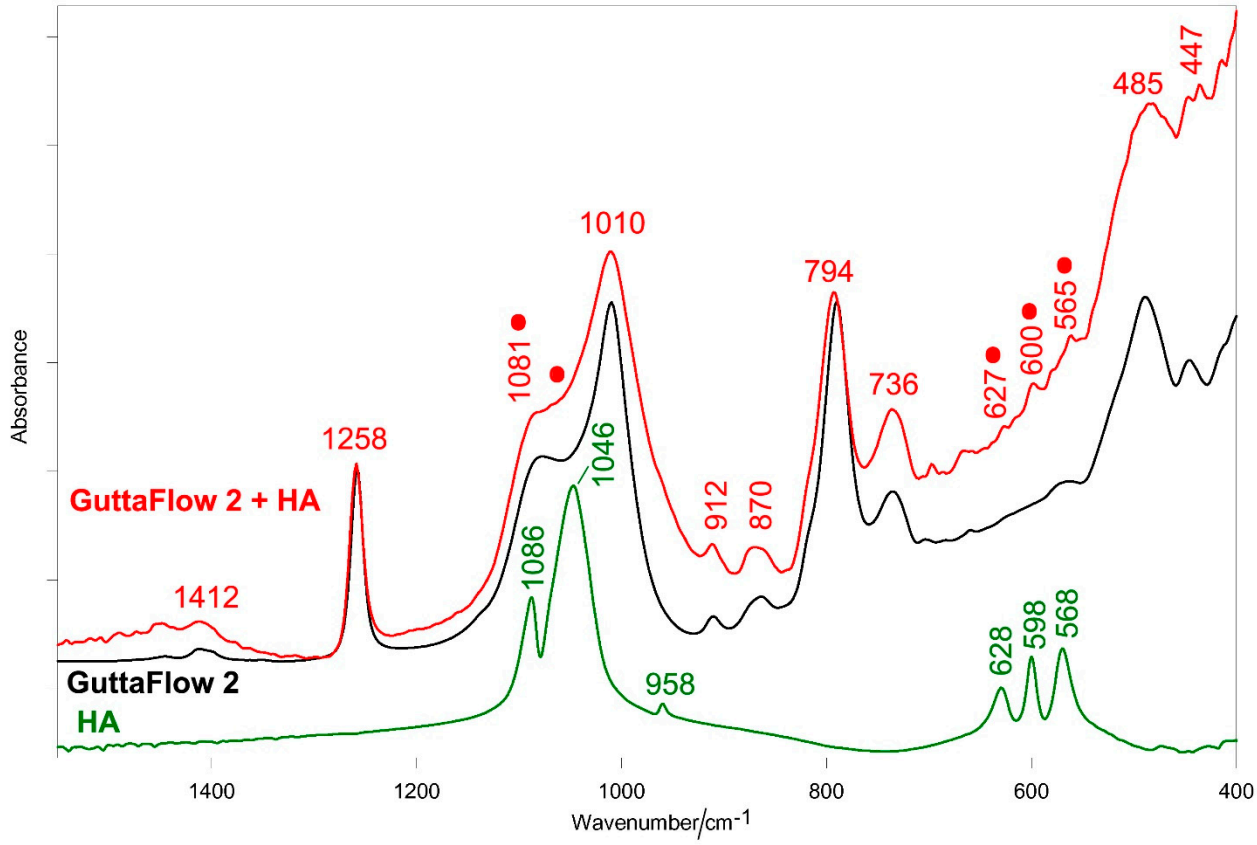

Figure S11. Average IR spectra of fresh GuttaFlow 2 + 20% HA and Guttaflow 2, normalized to the absorbance of the 1258 cm^{-1} band. The spectrum of HA is reported for comparison; spectral features assignable to it are indicated with a circle.

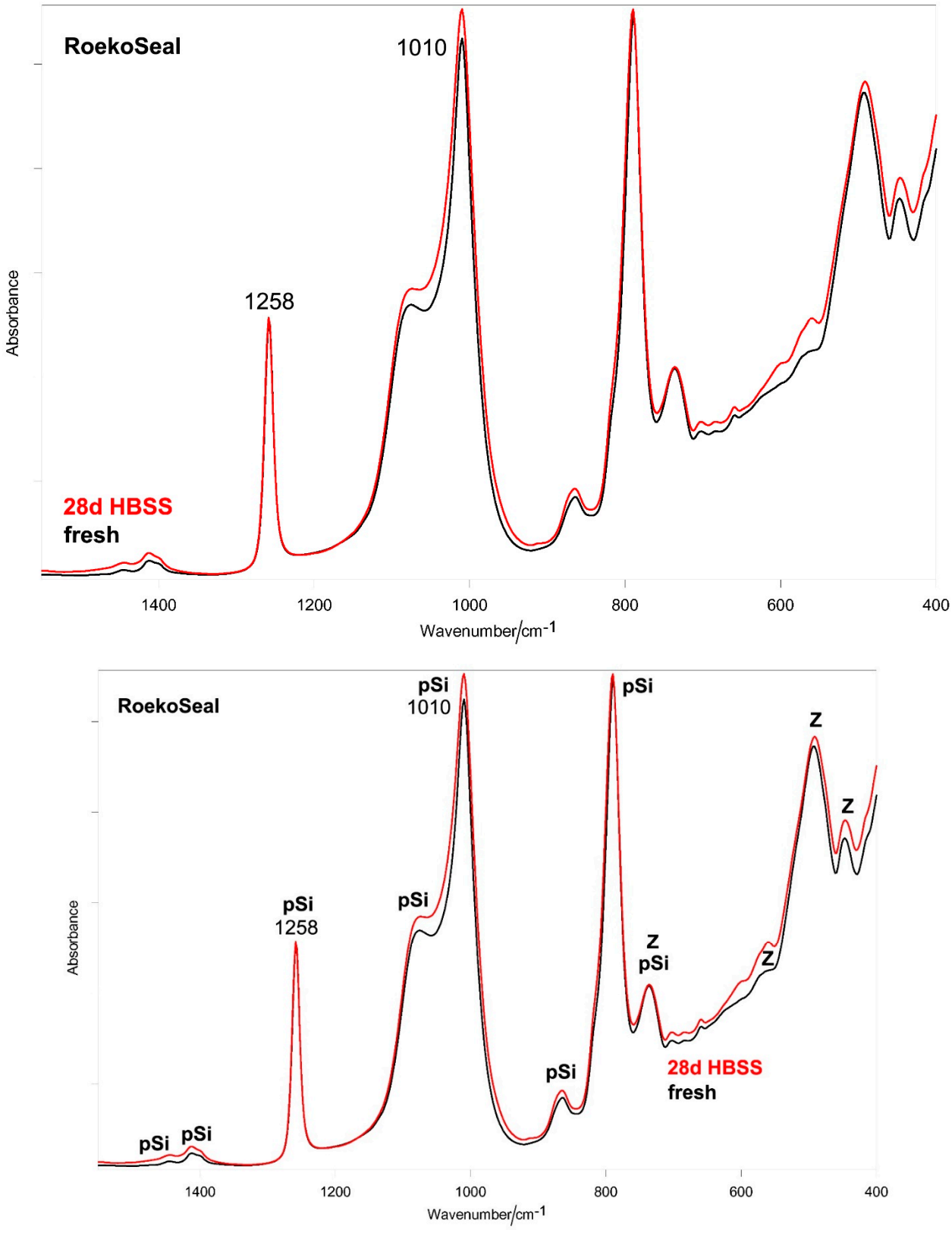

Figure S12. Average IR spectra recorded on the surface of RoekoSeal before (i.e. fresh) and after ageing in HBSS for 28 days. The spectra are normalized to the absorbance of the 1258 cm^{-1} band. The bands assignable to polydimethylsiloxane (pSi) and monoclinic zirconia (Z) are indicated.

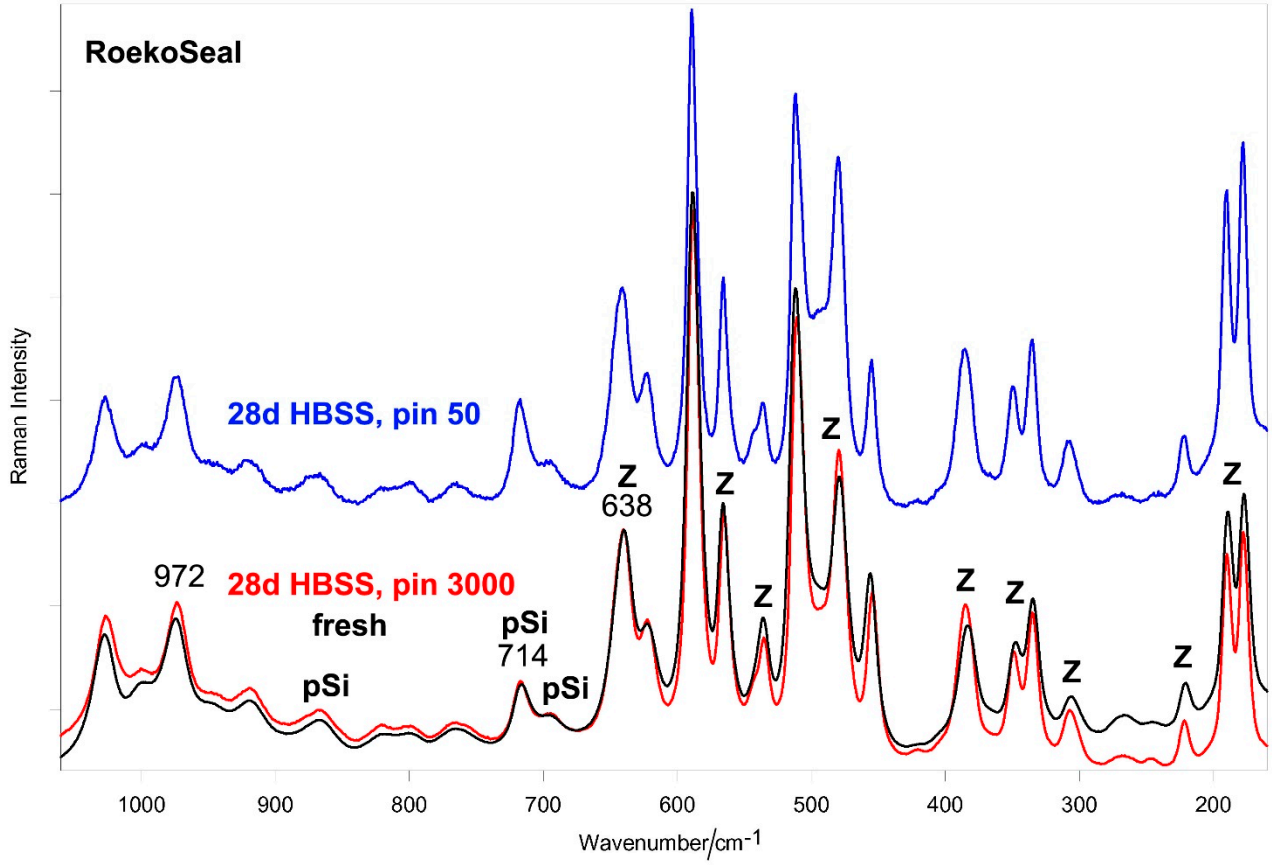

Figure S13. Average micro-Raman spectra recorded on the surface of RoekoSeal before (i.e. fresh) and after ageing in HBSS for 28 days. The spectra are normalized to the intensity of the 638 cm^{-1} band. The spectra on the aged sample were recorded using pinholes of 3000 µm (pin 3000) and 50 µm (pin 50). The bands assignable to monoclinic zirconia (Z) and polydimethylsiloxane (pSi) are indicated.

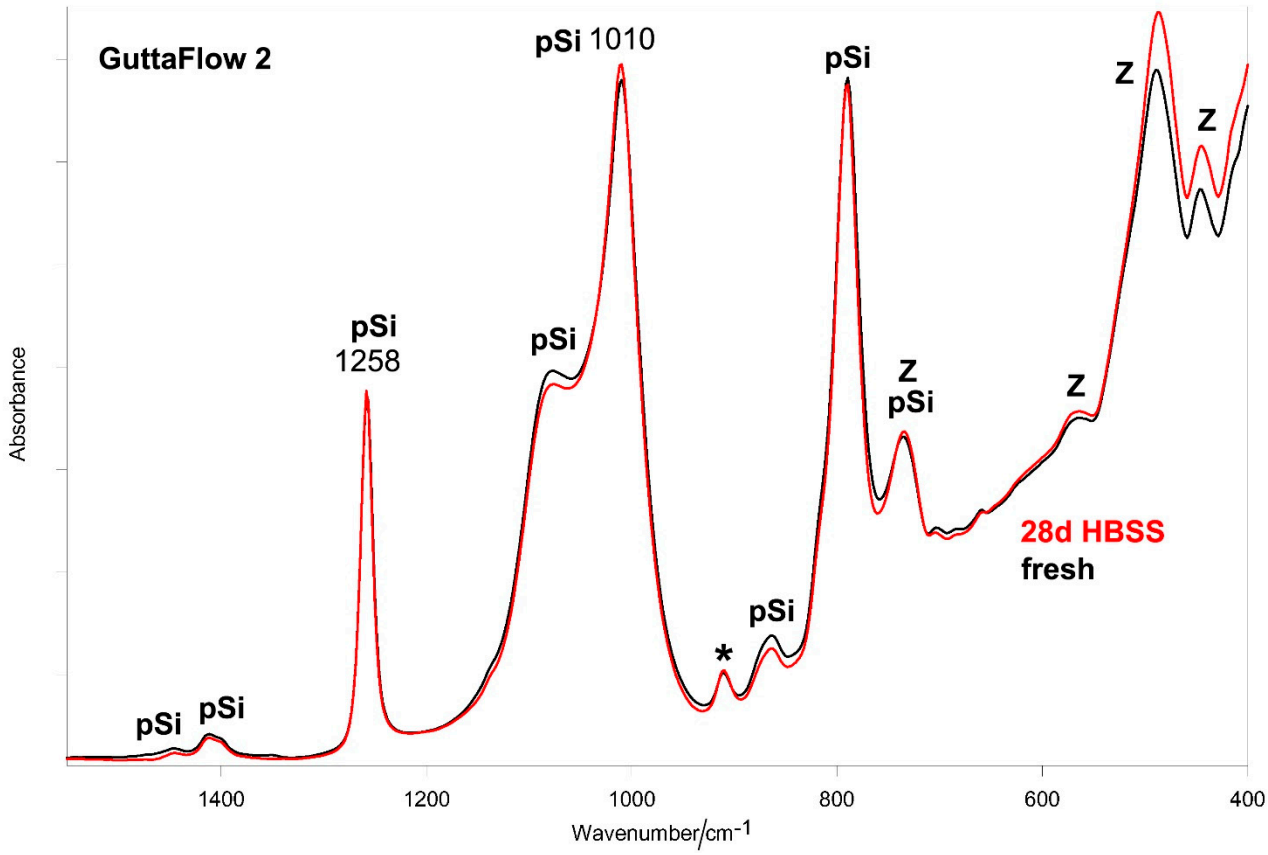

Figure S14. Average IR spectra recorded on the surface of GuttaFlow 2 before (i.e. fresh) and after ageing in HBSS for 28 days. The spectra are normalized to the absorbance of the 1258 cm^{-1} band. The bands assignable to polydimethylsiloxane (pSi) and monoclinic zirconia (Z) are indicated together with those specifically assigned to unreacted Si-H bonds (*).

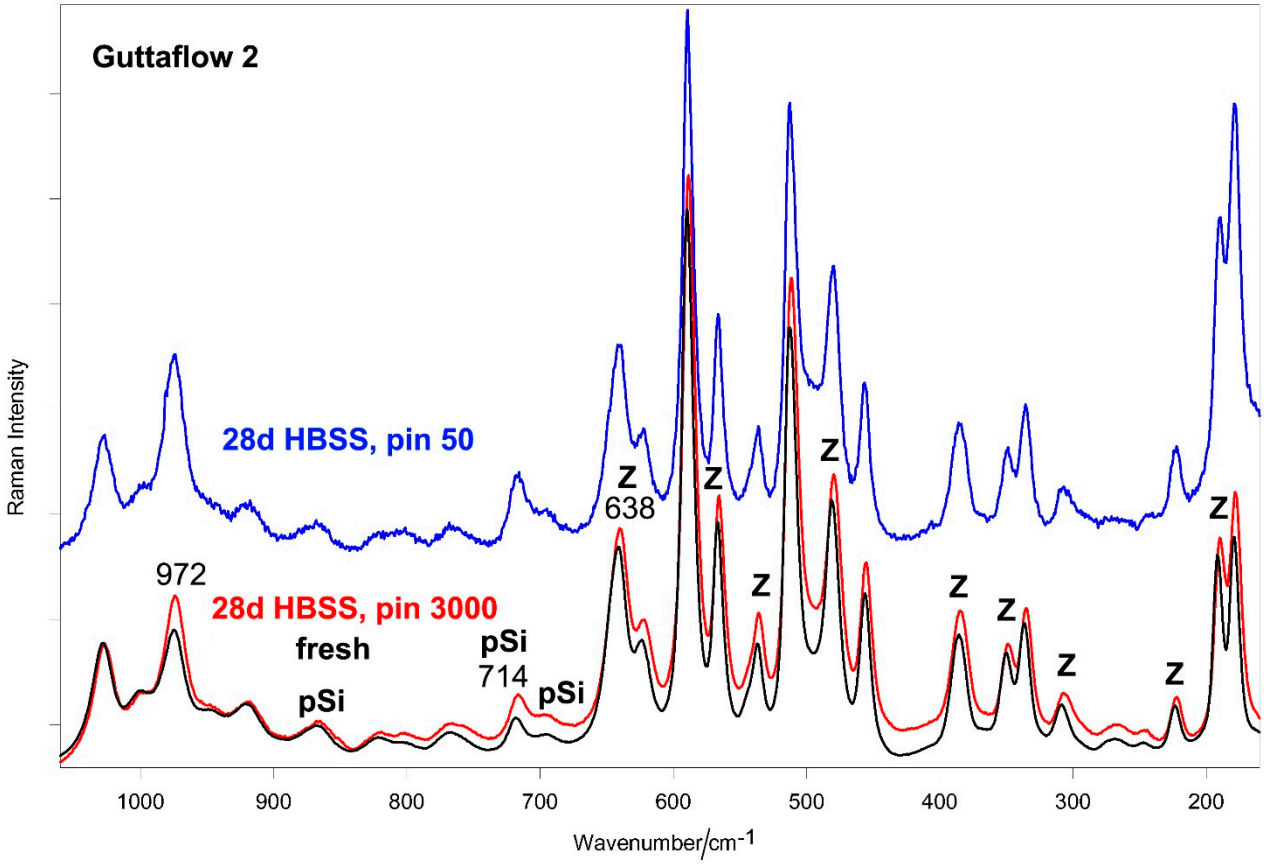

Figure S15. Average micro-Raman spectra recorded on the surface of GuttaFlow 2 before (i.e. fresh) and after ageing in HBSS for 28 days. The spectra on the aged sample were recorded using pinholes of 3000 µm (pin 3000) and 50 µm (pin 50). The bands assignable to monoclinic zirconia (Z) and polydimethylsiloxane (pSi) are indicated.

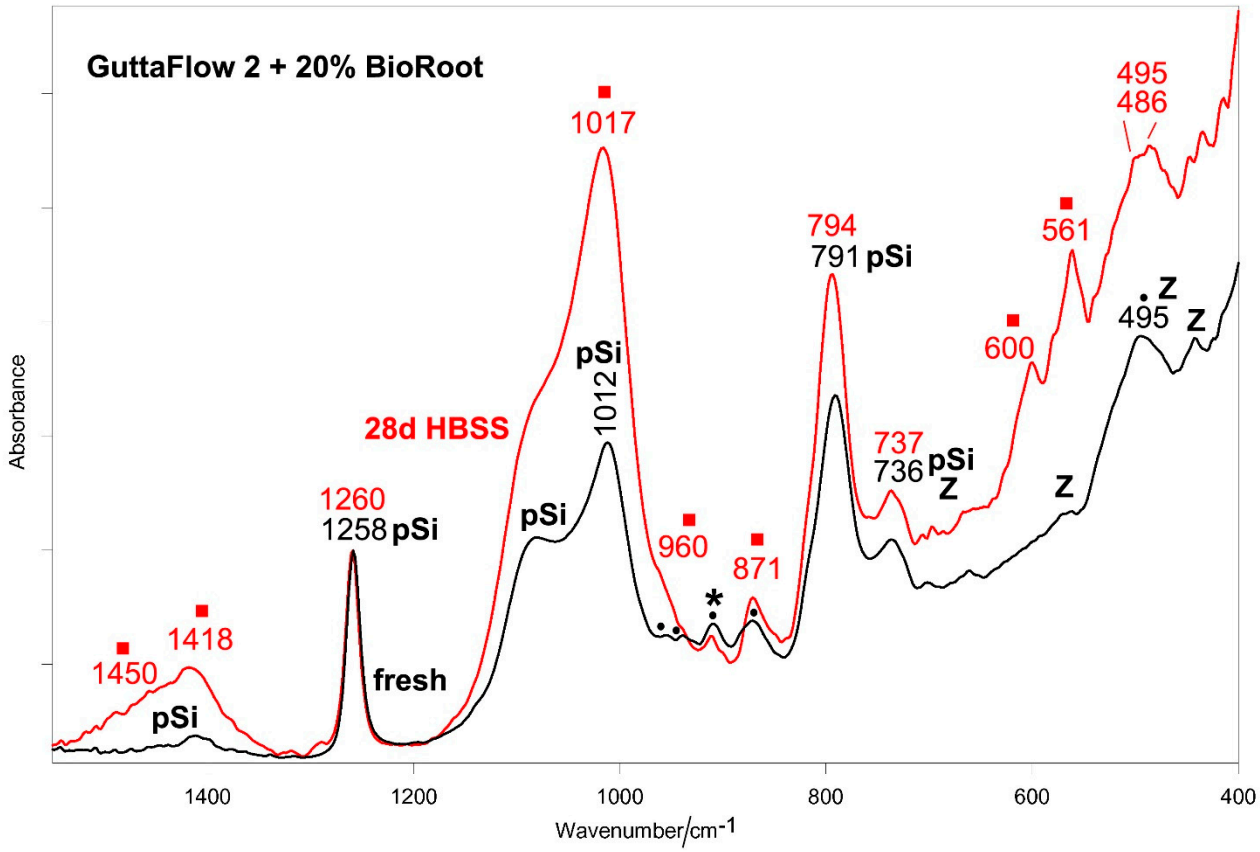

Figure S16. Average IR spectra recorded on the surface of GuttaFlow 2 + 20% BioRoot RCS, before (i.e., fresh) and after ageing in HBSS for 28 days. The spectra are normalized to the absorbance of the 1258 cm^{-1} band. The bands assignable to BioRoot RCS doping mineralizing agent (●) and B-type carbonated apatite (■) are indicated together with those of polydimethylsiloxane (pSi), monoclinic zirconia (Z) and unreacted Si-H bonds (*).

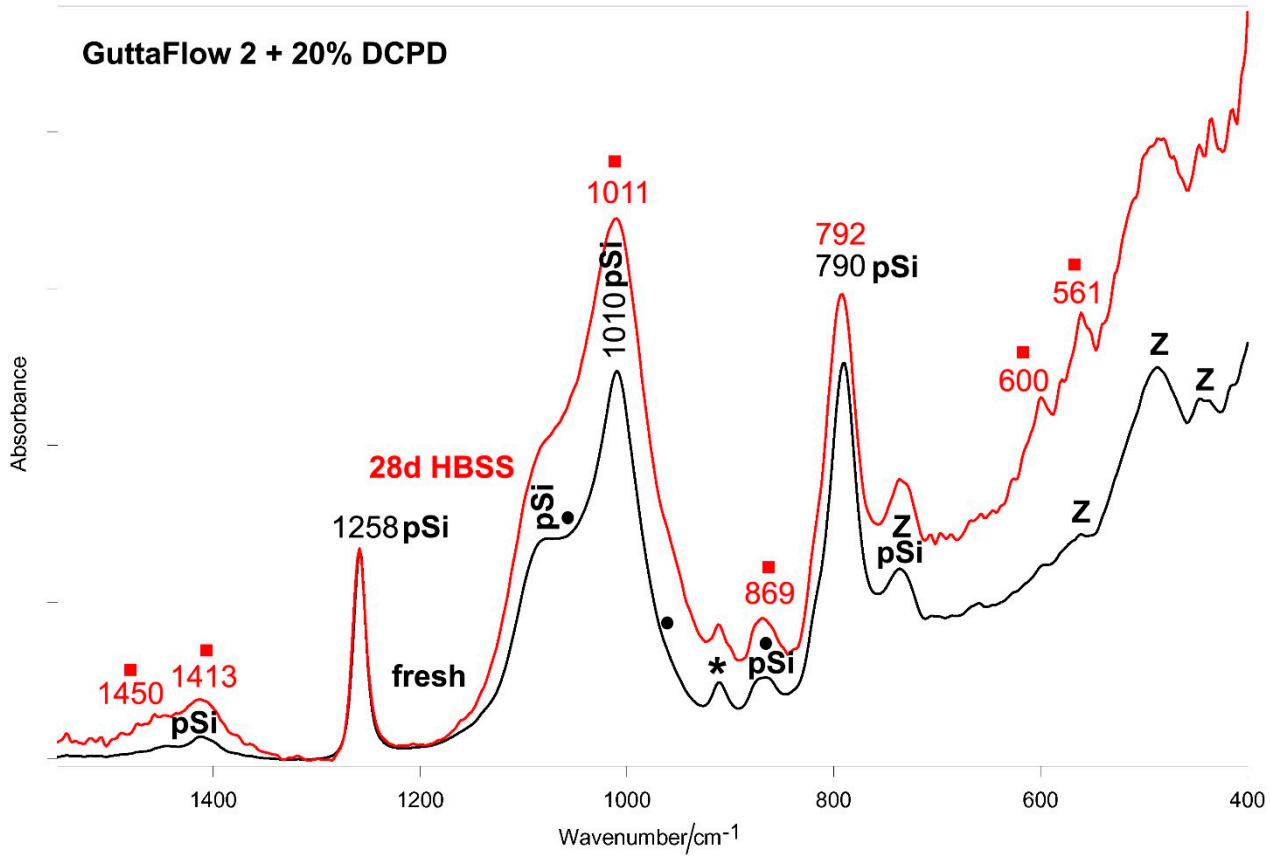

Figure S17. Average IR spectra recorded on the surface of GuttaFlow 2 + 20% DCPD, before (i.e., fresh) and after ageing in HBSS for 28 days. The spectra are normalized to the absorbance of the 1258 cm^{-1} band. The bands assignable to DCPD doping mineralizing agent (●) and B-type carbonated apatite (■) are indicated together with those of polydimethylsiloxane (pSi), monoclinic zirconia (Z) and unreacted Si-H bonds (*).

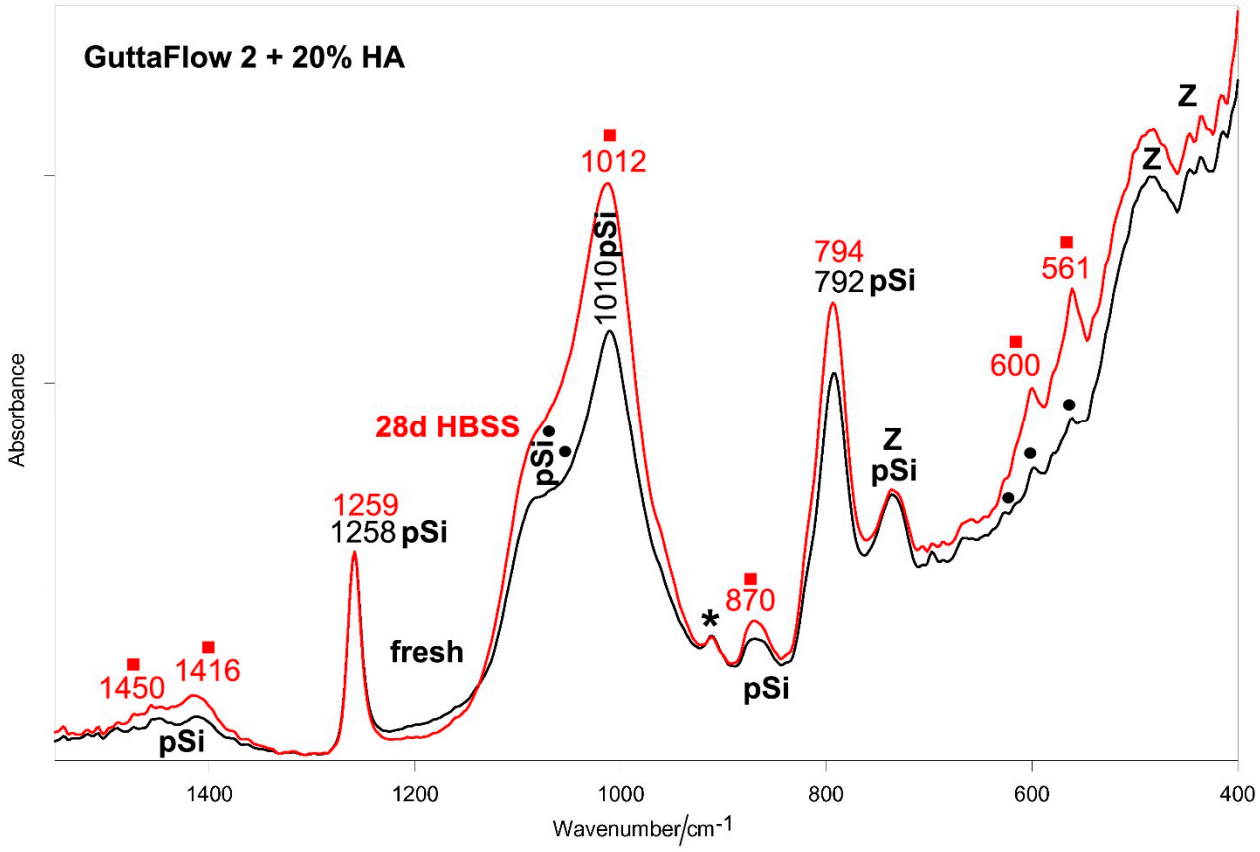

Figure S18. Average IR spectra recorded on the surface of GuttaFlow 2 + 20% HA, before (i.e., fresh) and after ageing in HBSS for 28 days. The spectra are normalized to the absorbance of the 1258 cm^{-1} band. The bands assignable to HA doping mineralizing agent (●) and B-type carbonated apatite (■) are indicated together with those of polydimethylsiloxane (pSi), monoclinic zirconia (Z) and unreacted Si-H bonds (*).

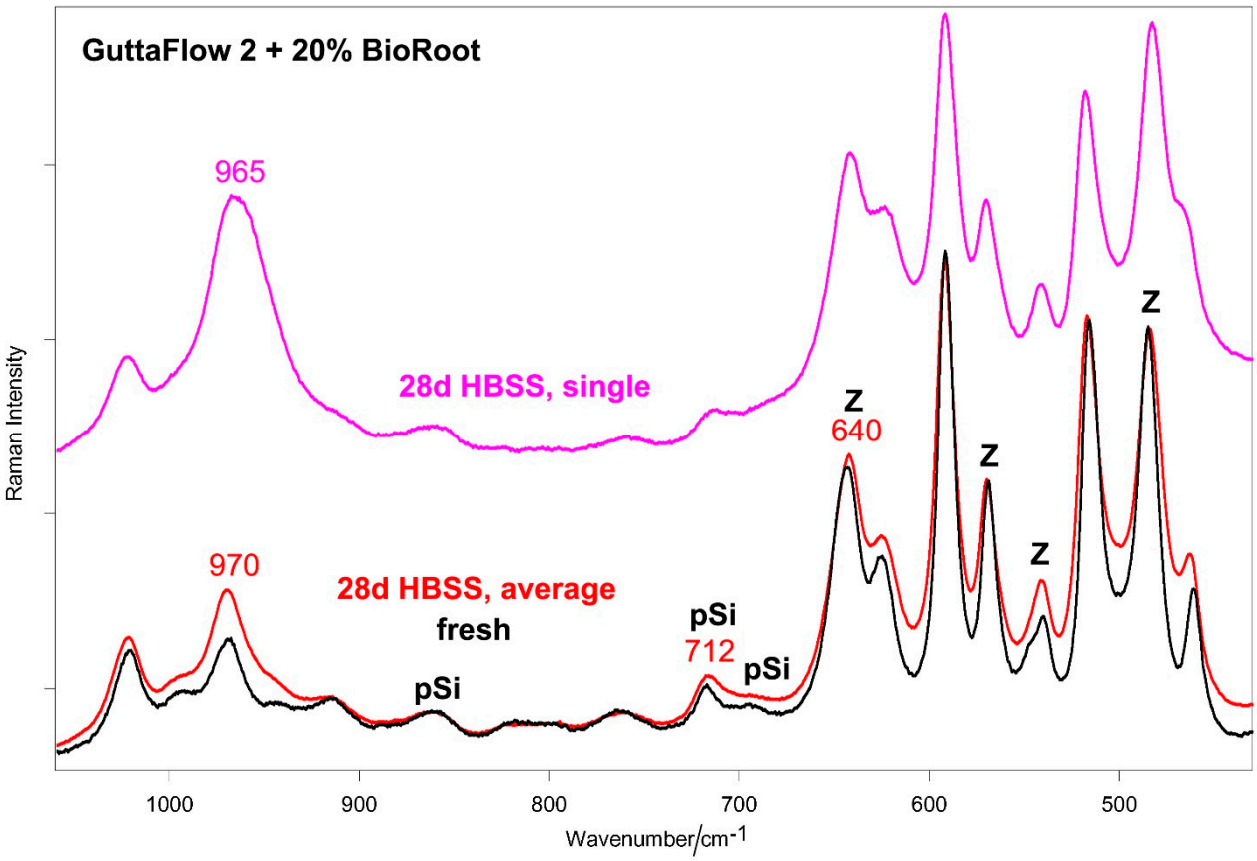

Figure S19. Average micro-Raman spectra recorded on the surface of GuttaFlow 2 + 20% BioRoot RCS, before (i.e. fresh) and after ageing in HBSS for 28 days. The spectra are normalized to the intensity of the 638 cm^{-1} band. A single spectrum is shown as well (i.e. that recorded in the position that among those analysed revealed the thickest deposit). The bands assignable to monoclinic zirconia (Z) and polydimethylsiloxane (pSi) are indicated.

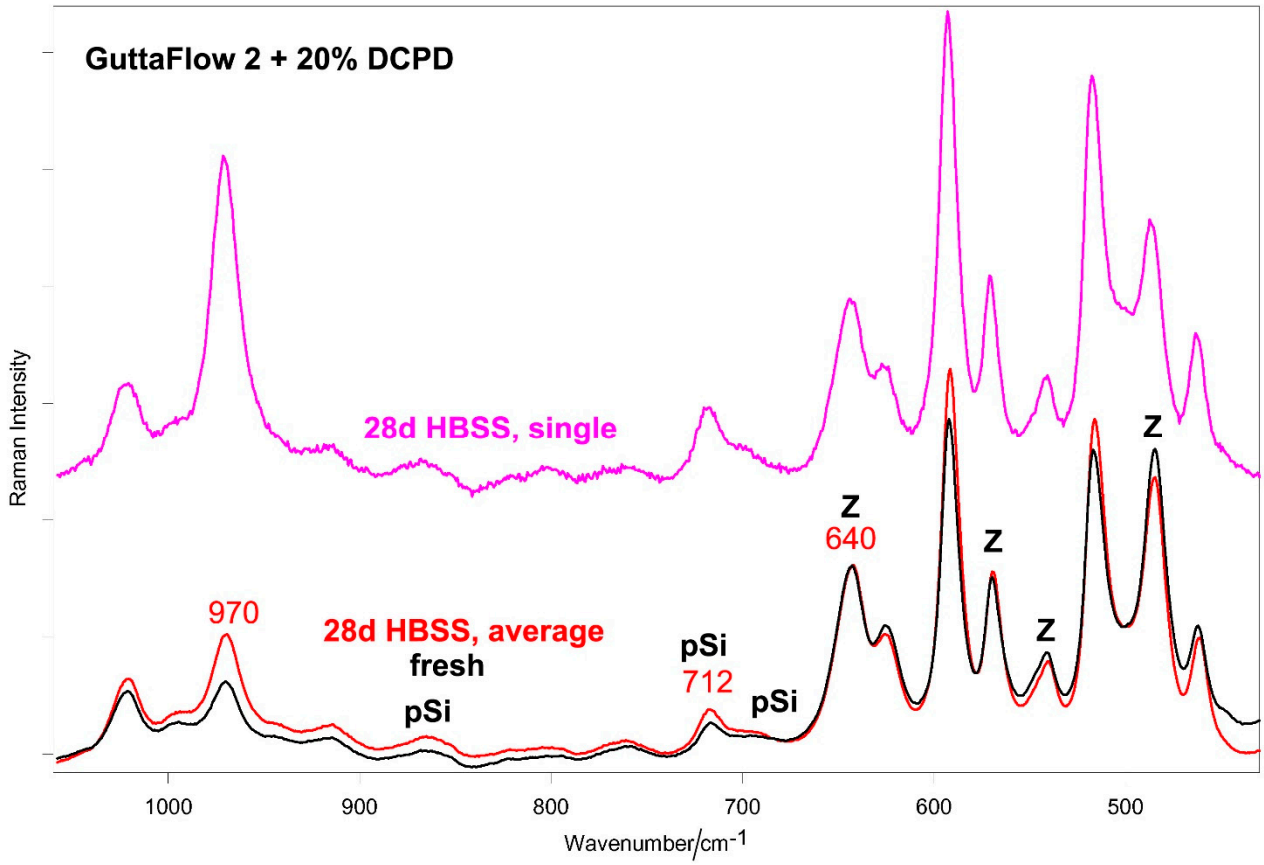

Figure S20. Average micro-Raman spectra recorded on the surface of GuttaFlow 2 + 20% DCPD, before (i.e. fresh) and after ageing in HBSS for 28 days. The spectra are normalized to the intensity of the 638 cm^{-1} band. A single spectrum is shown as well (i.e. that recorded in the position that among those analysed revealed the thickest deposit). The bands assignable to monoclinic zirconia (Z) and polydimethylsiloxane (pSi) are indicated.

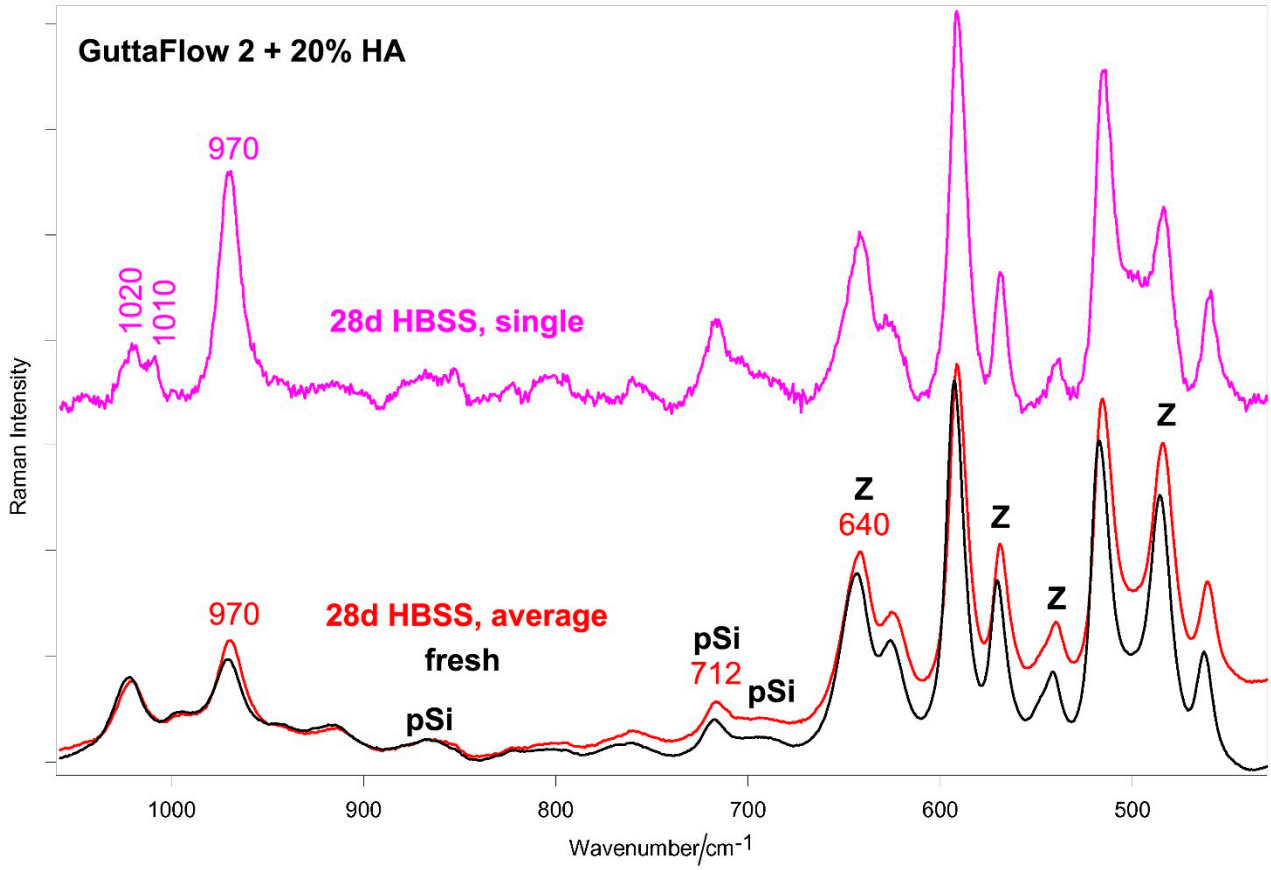

Figure S21. Average micro-Raman spectra recorded on the surface of GuttaFlow 2 + 20% HA, before (i.e. fresh) and after ageing in HBSS for 28 days. The spectra are normalized to the intensity of the 638 cm^{-1} band. A single spectrum is shown as well (i.e. that recorded in the position that among those analysed revealed the thickest deposit). The bands assignable to monoclinic zirconia (Z) and polydimethylsiloxane (pSi) are indicated.